ELSEVIER

Journal of Nuclear Materials 313–316 (2003) 1119–1122

journal of nuclear materials

www.elsevier.com/locate/jnucmat

Particle-in-cell simulations of the plasma-wall transition with a magnetic field almost parallel to the wall

D. Tskhakaya *, S. Kuhn

Plasma and Energy Physics Group, Association Euratom ÖAW, Technikerstrasse 25/II, Department of Theoretical Physics, University of Innsbruck, A-6020 Innsbruck, Austria

Abstract

Using simple analyses and 1d3v (one space and three velocity dimension) particle-in-cell simulations we show that the properties of the plasma-wall transition change when the angle α between the wall and the magnetic field is of the order of, or smaller than, certain values α_1, α_2. These values depend on the ion mass and collisionality, and on the ion-to-electron temperature ratio in the magnetic presheath. In this range of α, no significant decrease in the particle and heat fluxes to the wall is expected with decreasing α.

PACS: 52.40.Hf; 52.55.Fa; 52.65.Pr
Keywords: Plasma sheath; Presheath; Plasma-wall interaction; PIC simulations

1. Theory

In the design of contemporary and future fusion devices, there is a clear tendency to decrease the inclination angle α between the divertor plates and the magnetic field. It is assumed that the undesirable particle and energy fluxes decrease with decreasing α. On the other hand, up to now it was unclear whether for extremely low angles ($\alpha \lesssim 1°$) the 'classical' plasma-wall transition (PWT) exists. There are two reasons for this: First, at these angles the ion flux becomes 'scraping-off'-dominated and the potential drop across the PWT may therefore differ from the classical one [1,2]. Second, the projection of the charged-neutral-collision mean free path onto the normal to the wall can become of the same order as the ion gyroradius, so that the assumption of a collisionless magnetic presheath (MP) is no longer valid [1,2].

In describing the PWT it is (usually) assumed that $\lambda_D \ll \rho_i \ll l_{cnc} \ll l_{cc}$ (see Fig. 1), where λ_D is the Debye length, ρ_i is the ion Larmor radius, and l_{cnc} and l_{cc} are the charged-neutral particle and the Coulomb collision mean free paths, respectively. Then the PWT is free of Coulomb collisions and can be divided into three parts [1]: the Debye sheath (DS), the MP and the collisional presheath (CP). The collisionless DS (width is a few λ_D) forms just in front of the wall and is characterized by a strong space charge. In the quasineutral collisionless MP (width is a few ρ_i), the ion scraping-off and the related kinetic effects become important. In the CP (extension along the normal to the wall is about $l_{cnc}\sin\alpha$), the collision effects become dominant. This subdivision allows us to consider different parts of the PWT separately. Following this strategy, we present some (well known) results for the PWT with inclination angle above the critical α (see for example [1,2]).

The main characteristics of the DS and the MP are the potential drop between the MP entrance (MPE), associated with the boundary between the MP and CP, and the wall ($\Delta\phi_{MP}$), the normal (to the wall) component of the ion fluid velocity at the MPE ($V_{x,MP}$), and the electron and the ion heat transmission coefficients (γ_e, γ_i):

* Corresponding author. Permanent address: Institute of Physics, Georgian Academy of Sciences, Tbilisi, Georgia.
E-mail address: david.tskhakaya@uibk.ac.at (D. Tskhakaya).

0022-3115/03/$ - see front matter
PII: S0022-3115(02)01548-9

$$\Delta\phi_{\mathrm{MP}} = \frac{T_\mathrm{e}}{2e}\ln\frac{M_\mathrm{i}}{2\pi m_\mathrm{e}}\frac{T_\mathrm{e}}{T_\mathrm{e}+T_\mathrm{i}}, \tag{1}$$

$$V_{x,\mathrm{MP}} = c_\mathrm{s}\sin\alpha = \sqrt{\frac{T_\mathrm{e}+T_\mathrm{i}}{M_\mathrm{i}}}\sin\alpha, \tag{2}$$

$$\gamma_\mathrm{e} = \frac{\Theta_\mathrm{e}}{T_\mathrm{e}\Gamma_\mathrm{e}} = 2 + \frac{e\Delta\phi_{\mathrm{MP}}}{T_\mathrm{e}} \approx 5, \quad \gamma_\mathrm{i} = \frac{\Theta_\mathrm{i}}{T_\mathrm{i}\Gamma_\mathrm{i}} = 2.0\text{–}3.5. \tag{3}$$

These values define the particle and heat fluxes to the wall and are used for the boundary conditions in fluid codes simulating different plasma devices. For simplicity, we consider in (1) just the floating case. Here e is the electron charge, m_e and M_i are the electron and ion masses, and T_s, Γ_s and Θ_s are the electron (s = e) and the ion (s = i) temperatures, particle fluxes and heat fluxes at the MPE, respectively.

The CP is characterized by the potential drop across it $\Delta\phi_{\mathrm{CP}}$. The heat flux in the CP strongly depends on the collision processes inside it, which makes it inconvenient to introduce corresponding heat transmission coefficients, as is done for the collisionless MP. Assuming that the electrons are Boltzmann-distributed, one obtains the density (n_{MP}) and the ion flux (Γ_{MP}) at the MPE as

$$n_{\mathrm{MP}} = n_0\exp(-e\Delta\phi_{\mathrm{CP}}/T_\mathrm{e}), \quad \Gamma_{\mathrm{MP}} = n_{\mathrm{MP}}V_{\mathrm{MP}};$$

here, n_0 is the density at the entrance of the CP (associated with the core plasma side boundary of the CP).

In order to obtain $\Delta\phi_{\mathrm{CP}}$ we consider the ion continuity and momentum conservation equations [7,8]:

$$\frac{\partial}{\partial x}n\upsilon = n\frac{\nu_\mathrm{i}}{\sin\alpha},$$
$$\upsilon\frac{\partial}{\partial x}\upsilon + \frac{e}{M_\mathrm{i}}\frac{\partial}{\partial x}\phi = -\frac{1}{nM_\mathrm{i}}\frac{\partial}{\partial x}nT_\mathrm{i} - \upsilon\frac{\nu_\mathrm{i}+\nu_{\mathrm{mt}}}{\sin\alpha}; \tag{4}$$

here ν_i and ν_{mt} are the electron impact ionization and the ion-neutral momentum transfer collision frequencies, respectively, υ is the ion parallel (to the magnetic field) fluid velocity, and ϕ is the potential.

By neglecting temperature gradients inside the CP and assuming that the electrons are Boltzmann-distributed, we solve the system (4) to obtain

$$\Delta\phi_{\mathrm{CP}} = \frac{T_\mathrm{e}}{e}\frac{\nu_\mathrm{i}+\nu_{\mathrm{mt}}/2}{\nu_\mathrm{i}+\nu_{\mathrm{mt}}}\ln\frac{2\nu_\mathrm{i}+\nu_{\mathrm{mt}}}{\nu_\mathrm{i}+(\nu_\mathrm{i}+\nu_{\mathrm{mt}})(\upsilon_0/c_\mathrm{s})^2}, \tag{5}$$

where υ_0 is the ion parallel velocity at the entrance of the CP.

We note that in deriving (5) we do not use any assumption about the angle α, hence, the expression (5) should be valid for any α. In contrast to (5), all the expressions (1)–(3) have been obtained with assumptions which cannot be satisfied for very small α. In order to demonstrate this, we introduce two critical angles:

$$\alpha_1 = \sqrt{\frac{T_\mathrm{i}}{T_\mathrm{e}}\frac{m_\mathrm{e}}{M_\mathrm{i}}}, \quad \alpha_2 = \frac{\nu_\mathrm{i}+\nu_{\mathrm{mt}}}{\Omega}, \tag{6}$$

where $\Omega = eB/M_\mathrm{i}$ is the ion cyclotron frequency. For convenience, we will henceforth refer to the PWT as classical PWT when $\alpha \gg \alpha_1, \alpha_2$.

It is easy to see that, if $\alpha \lesssim \alpha_1$, the electron convective flux to the wall, $\sim nV_T^\mathrm{e}\sin\alpha \approx nV_T^\mathrm{e}\alpha$, is of the same order as, or less than, the ion scraping-off flux [4], $\sim nV_T^\mathrm{i}\cos\alpha \approx nV_T^\mathrm{i}$ ($V_T^{\mathrm{i,e}} = \sqrt{T_{\mathrm{i,e}}/m_{\mathrm{i,e}}}$). Thus, no potential drop is required inside the MP in order to reduce the electron flux to the wall and, in principle, the potential profile need not be of the monotonically decreasing shape usually encountered.

If $\alpha \lesssim \alpha_2$, then (a) the width of the MP, $\sim\rho_\mathrm{i} = V_T^\mathrm{i}/\Omega$, becomes of the order of the projection on the normal to the wall of the collision mean free path, $\sim l_{\mathrm{cnc}}\sin\alpha \sim V_T^\mathrm{i}\alpha/(\nu_\mathrm{i}+\nu_{\mathrm{mt}})$. Hence, the assumption of the collisionless MP no longer valid. (b) The 'collisional' part of the normal (to the wall) component of the ion fluid velocity (V_x^{col}) at the MPE cannot be neglected with respect to the projection of the ion parallel (to the magnetic field) velocity on the normal to the wall,

$$V_x^{\mathrm{col}} \gtrsim \upsilon\sin\alpha \approx c_\mathrm{s}\alpha. \tag{7}$$

Hence, the ion fluid velocity at the MPE is not directed along the magnetic field:

$$V_{x,\mathrm{MP}} \approx V_x^{\mathrm{col}} + c_\mathrm{s}\sin\alpha \neq c_\mathrm{s}\sin\alpha, \tag{8}$$

and the Bohm–Chodura condition (1) is not satisfied any more.

The collisional velocity, V_x^{col}, results from the collisions with neutrals. In order to estimate V_x^{col} and prove (7), we consider ion continuity and momentum conservation equations for the MP and neglect terms of the order of α [7]:

$$\frac{\partial}{\partial x}nV_x = \nu_\mathrm{i}n, \quad V_x\frac{\partial}{\partial x}V_y = -\Omega V_x - \nu_{\mathrm{mt}}V_y,$$
$$V_x\frac{\partial}{\partial x}V_x = -\frac{e}{M_\mathrm{i}}\frac{\partial}{\partial x}\phi + \Omega V_y - \frac{1}{M_\mathrm{i}n}\frac{\partial}{\partial x}nT_\mathrm{i} - (\nu_\mathrm{i}+\nu_{\mathrm{mt}})V_x. \tag{9}$$

Here V_x and V_y are the normal and parallel to the wall components of the ion fluid velocity. As was done for the CP, we neglect temperature gradients and assume that the electrons are Boltzmann-distributed. Taking into the account that for magnetized plasmas ν_{mt}, $\nu_\mathrm{i} \ll \Omega$, and neglecting terms of the order $\sim V_x/c_\mathrm{s}$, $V_y/c_\mathrm{s} \ll 1$, we write the solution of the system (9) near the MPE in the form

$$V_x \approx v_{\mathrm{mt}} \frac{c_s^2}{\Omega^2} \frac{1}{x_0 - x}, \quad x_0 = \mathrm{const} > x, \quad v_i = 0;$$
$$V_x \approx \sqrt{\frac{v_i + v_{\mathrm{mt}}}{v_i}} \frac{c_s^2}{\Omega^2} \cot\left[\sqrt{\frac{v_i}{v_i + v_{\mathrm{mt}}}} \frac{\Omega}{c_s} \frac{1}{x_0 - x}\right], \quad v_i \neq 0. \tag{10}$$

Taking into the account that the gradient scale length in the MP is of the order of ρ_i, we get from (10)

$$V_x^{\mathrm{col}} \sim V_{x,\mathrm{MP}}(\alpha = 0) \sim c_s \frac{v_i + v_{\mathrm{mt}}}{\Omega}, \tag{11}$$

which agrees with the condition (7).

These analyses show that properties of the PWT for a very small α can be different from the properties of the classical PWT. Previous investigations of the PWT with an extremely small α did not give a unique result: (i) in [3] the author assumed that the potential profile may be not only be decreasing, but also increasing (!); (ii) in [5,6], the authors used a monotonically decreasing potential, and (iii) in [4] a non-monotonic potential profile has been obtained. Probably, these discrepancies result from the different assumptions made in these papers.

The aim of the present work is to make self-consistent simulations of the PWT for subcritical angles α, and to obtain its main characteristics.

2. Simulations

For the particle-in-cell (PIC) simulations we use the 1d3v code BIT1 [8] developed on the basis of the code XPDP1 from Berkeley [9].

The simulation geometry is shown in Fig. 1. In the center of the simulation domain we implemented an ambipolar particle (ion and electron) source. In order to keep the particle distribution in this region close to Maxwellian, we used the following mechanism: during their stay inside the source region, the velocity of every particle will artificially change at least once. The substituted velocities are Maxwell-distributed. This mechanism is equivalent to simplified Coulomb collisions. At each side of the system we have an absorbing wall. The motion of ions and electrons is fully resolved in space and time.

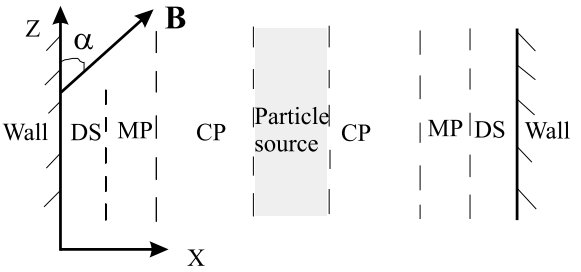

Fig. 1. Simulation geometry.

We consider a hydrogen plasma. The plasma parameters are chosen so as to be relevant to tokamak parameters.: $B = 1$ T, $n \sim 10^{18}$ m^{-3} and $T_{i,e} \sim 30$ eV. For the charged-neutral particle collisions we consider the ionic hydrogen elastic and charge-exchange collisions with atomic hydrogen, and the electron – atomic hydrogen elastic, excitation and ionization collisions [10]. The related cross sections are taken from [11]. The atomic-hydrogen fraction represents a fixed background. In order to insure high accuracy, a very large number of simulation particles is used, on average about 500 per spatial grid cell. During the simulation, Maxwell-distributed electrons and ions are injected into the source region. After a few ion transit times ($L/\sin\alpha \sqrt{T_i/M_i}$), the system reaches a stationary state.

Four simulations have been made, two with $\alpha = 1°$ and two with $\alpha = 0.5°$. For each α we consider cases of

Table 1
Plasma parameters

Run		1	2	3	4
α		1°	1°	0.5°	0.5°
α_1		0.52°	0.8°	0.57°	0.86°
α_2		0.24°	0.06°	0.12°	0.03°
$e\Delta\phi_{\mathrm{MP}}/T_e$	Simulation	2.0 ± 0.2	2.1 ± 0.1	2.1 ± 0.1	2.2 ± 0.1
	Analytic	2.8	2.7	2.8	2.7
$e\Delta\phi_{\mathrm{CP}}/T_e$	Simulation	1.7 ± 0.2	1.1 ± 0.1	1.8 ± 0.1	0.9 ± 0.1
	Analytic	1.7	0.9	1.6	1.0
γ_e	Simulation	4.0 ± 0.3	4.1 ± 0.3	4.1 ± 0.3	4.2 ± 0.2
	Analytic	4.8	4.7	4.8	4.7
γ_i	Simulation	6.4 ± 2.3	4.7 ± 1.3	5.6 ± 1.8	3.7 ± 1.4
	Analytic	2.0–3.5	2.0–3.5	2.0–3.5	2.0–3.5
$V_{x,\mathrm{MP}}$ (km/s)	Simulation	1.6 ± 0.1	1.2 ± 0.1	0.7 ± 0.2	5 ± 0.1
	Analytic, from (2)	1.0	1.1	0.5	0.5
	Analytic, from (8)	1.2	1.1	0.6	0.5

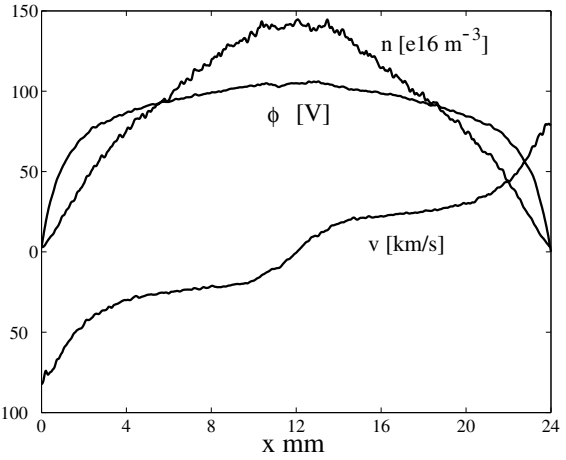

Fig. 2. Profiles of the potential ϕ, the ion density n and the ion parallel velocity v (run 2).

low and high collisionality. In the latter, the electron-neutral collisions have not been considered.

Our simulations show that for very small α the PWT qualitatively has the same features as the classical one: it consists of the DS, MP and CP and the plasma parameters have smooth, monotonic profiles. The simulation results are summarized in Table 1. As an example, the profiles of the plasma parameters (averaged over a few tens of plasma oscillation periods) for run 2 are plotted in the Fig. 2. For comparison we also give analytic results obtained from Eqs. (1)–(3) and (5). In the simulation the MPE was recognized as a point where the ion parallel velocity v was equal to c_s (typically, a few ion gyroradii away from the wall).

As we see from Table 1, the CP does not change its properties for the critical α, while, as was to be expected, the MP characteristics differ from those for the classical PWT in that $\Delta\phi_{MP}$, $V_{x,MP}$ and γ_i are higher than ones obtained from Eqs. (1)–(3). The condition $\alpha_1 > \alpha_2$, which is satisfied in all our simulations, does not allow us to estimate the relative role of each of these critical angles. Still, we can conclude that for $\alpha \sim \alpha_1$ the potential drop $\Delta\phi_{MP}$ is significantly reduced (runs 1–4), while for $\alpha \sim \alpha_2$ the quantities $V_{x,MP}$ and γ_i are higher than the classical ones (runs 1 and 3).

3. Summary

For critical angles α ($\alpha \lesssim \alpha_1$ or $\alpha \lesssim \alpha_2$) the PWT is, in general, different from the classical one. The potential and density profiles decrease monotonically towards the wall (in agreement with results from [6,7]), but the potential drop across the MP cannot be approximated as in (11). The ion fluid velocity is not directed along the magnetic field and the Bohm–Chodura condition (2) is not satisfied at the MPE. The ion heat transmission coefficient γ_i is larger than the classical one.

According to our results, we propose to use in the case of critical α the expression (8) (with V_x^{col} from (11)), rather than the Bohm–Chodura condition (2), as plasma-wall boundary conditions the fluid codes.

Finally it is important to note that, according to (11),

$$V_{x,MP} > V_{x,MP}(\alpha = 0) \sim \frac{v_i + v_{mt}}{\Omega} c_s.$$

Hence, with α decreasing below the critical value we should not expect a significant decrease in the ion flux and the ion heat flux to the wall. The minimum values of these fluxes are given by

$$\Gamma_i^{min} \approx \frac{v_i + v_{mt}}{\Omega} c_s n_{MP}, \quad \Theta_i^{min} = \gamma_i T_i \Gamma_i^{min}, \quad \gamma_i > 2.$$

Acknowledgements

This work was supported by Austrian Science Fund (FWF) Project P15013 and has been carried out within the Association Euratom-ÖAW. Its content is the sole responsibility of the authors and does not necessarily represent the views of the Commission or its services.

References

[1] K.-U. Riemann, J. Tech. Phys. 41 (2000) 89.
[2] P.C. Stangeby, The Plasma Boundary of Magnetic Fusion Devices, Institute of Physics Publishing, Bristol and Philadelphia, 2000.
[3] U. Daybelge, B. Bein, Phys. Fluids 24 (1981) 1190.
[4] R. Chodura, Europhys. Conf. Abstracts 16c, Pt. II (1992) 871.
[5] H. Schmitz, K.-U. Riemann, Th. Daube, Phys. Plasmas 3 (1996) 2486.
[6] Th. Daube, K.-U. Riemann, Phys. Plasmas 6 (1999) 2409.
[7] K.-U. Riemann, Phys. Plasmas 1 (1994) 552.
[8] D. Tskhakaya, S. Kuhn, Contribution Plasma Phys. 42 (2002) 302.
[9] J.P. Verboncoeur, M.V. Alves, V. Vahedi, C.K. Birdsall, J. Comput. Phys. 104 (1993) 321.
[10] C.K. Birdsall, IEEE Trans. Plasma Sci. 19 (1991) 65.
[11] R.K. Janev (Ed.), Atomic and Molecular Processes in the Fusion Edge Plasmas, Plenum, New York and London, 1995.